



Mechanical and durability analysis of geopolymer concrete incorporating bauxite residue, phosphogypsum, and ground granulated blast slag

Bheem Pratap¹ · Somenath Mondal¹ · B. Hanumantha Rao²

Received: 29 April 2023 / Accepted: 18 June 2023 / Published online: 25 June 2023
© The Author(s), under exclusive licence to Springer Nature Switzerland AG 2023

Abstract

One cementitious material is geopolymer concrete (GPC), which is produced by activating industrial by-products with alkaline activators. This study evaluates the mechanical and environmental properties of geopolymer concrete incorporating bauxite residue (BR) with phosphogypsum (PG) and ground granulated blast slag (GGBS). The compressive strength of GPC was 58.42 MPa at 28 days when BR was replaced with 10% PG and 30% GGBS. This indicates that the incorporation of PG and GGBS improved the strength development of GPC. The lowest charges passed, porosity, and water absorption of 1575 Coulombs, 7.53%, and 3.15%, respectively, were obtained when the bauxite residue was replaced with 10% phosphogypsum and 30% GGBS (B4). The scanning electron microscope (SEM) image shows that the 10% PG and 30% GGBS specimens exhibit a denser structure than the other specimens. This indicates that the PG and GGBS proportion has a substantial impact on the structure and strength of the GPC. These findings suggest that geopolymer concrete can be a promising alternative construction material that can contribute to sustainable development.

Keywords Geopolymer · Industrial by-products · Compressive strength · Durability · SEM

Introduction

The manufacture of conventional Portland cement—the binder used in concrete—requires high temperatures and energy consumption, which results in high carbon dioxide (CO₂) emissions (Reddy et al., 2020). In recent time, there has been an increasing attention in the development of alternative binders for concrete that can lessen the negative effect of cement industry (Naenudon et al., 2023). One of these alternatives is geopolymers. Geopolymers are inorganic

polymers synthesized from alumino-silicate precursors that can be activated by an alkaline solution (Pratap et al., 2023a, 2023b). The resulting material has a three-dimensional structure and shows good mechanical properties, chemical resistance, and fire resistance (Zakira et al., 2023). The precursor materials used for geopolymer production can include numerous industrial by-products such as GGBS, fly ash, PG, metakaolin and BR (Liu et al., 2022).

BR is a by-product of the alumina extraction process from bauxite ores. It is an alumina industry waste material that is produced around 120 million tons each year worldwide (Ma et al., 2022). BR contains high levels of iron oxide, highly alkaline, aluminum oxide, and silicon dioxide, which make it a potential precursor for geopolymer production. However, bauxite residue also contains several hazardous elements such as arsenic, chromium, and vanadium, which can be harmful to the ecosystem (Pratap et al., 2023a, b). In construction applications, BR-based geopolymer materials can be used to produce blocks, panels, and tiles, which have better insulation properties, reduced weight, and increased fire resistance. In refractory applications, red mud-based geopolymer materials can be used to produce high-temperature resistant materials that can be used in the steel and

✉ Bheem Pratap
2018rsce007@nitjsr.ac.in

Somenath Mondal
smondal.ce@nitjsr.ac.in

B. Hanumantha Rao
bhrao@iitbbs.ac.in

¹ Department of Civil Engineering, National Institute of Technology Jamshedpur, Jamshedpur, Jharkhand 831014, India

² School of Infrastructure, Indian Institute of Technology Bhubaneswar, Bhubaneswar, Odisha 752050, India

glass industries (Hoang et al., 2020). Geopolymerization of red mud involves the reaction between the alkaline activator solution and red mud, resulting in a solid material that can have comparable or better properties than traditional building materials (Toniolo et al., 2018). Additionally, geopolymerization of red mud can result in a material with improved mechanical strength, durability, and resistance to harsh environments (Zhang et al., 2020b). Overall, the use of BR as a geopolymer material can provide sustainable solutions to the growing demand for construction materials and can contribute to the decrease of waste generated from industrial processes (Jatoliya et al., 2023; Pratap et al., 2023a, b).

Phosphogypsum (PG) is another industrial by-products material generated through the manufacture of phosphoric acid from phosphate rock (Ren et al., 2023). It is a waste material that contains toxic, making its disposal challenging and expensive. However, PG contains significant amounts of calcium sulfate, which can be used as a source of sulfate ions in geopolymer production (Pratap et al., 2023a, b). Hence, it can also be used to create a geopolymer, a type of cement that is made from industrial waste and has many advantages over traditional Portland cement. Additionally, phosphogypsum-based geopolymer can be used to create decorative and architectural elements such as tiles, pavers and concrete (Meskini et al., 2022; Xu et al., 2022).

GGBS is a by-product produced during the production of iron in the blast furnace. GGBS has been used as an supplementary resource due to its excellent pozzolanic characteristics (Liang & Ji, 2021). Another significant benefit of using GGBS in geopolymer is that it enhances the workability of the mixture (Alam et al., 2019). GGBS improves the flow and decreases the viscosity of the geopolymer mixture, making it easier to pour and place. One of the primary uses of GGBS in geopolymer is to advance the strength and durability of GPC (Shahmansouri et al., 2021; Zhang et al., 2020a). GGBS is an excellent pozzolanic that reacts with calcium hydroxide to yield calcium aluminosilicate hydrate gel (C–A–S–H), which improves the strength and durability of geopolymer concrete (Nuaklong et al., 2019; Phumphan et al., 2018; Zhou et al., 2020).

Though these waste materials, at their individual level, have been utilized to a certain level to synthesize geopolymers, production of GPC using BR, PG and GGBS combination has not yet been attempted. As a result, the novelty of this study to evaluate the viability of BR-, PG- and GGBS-based geopolymer and to minimize cement usage is considered as a perspective idea. Keeping in mind coalesce among BR, PG and GGBS, an attempt is made to synthesize GPC using the combination of BR, PG and GGBS. One of the objectives of this research is to analyze the feasibility of the developed GPC for utilization in construction of pavement, taking into consideration factors such as mechanical properties, durability, and micro-characterization.

Materials and methods

This study utilized materials obtained from various sources. BR was obtained from HINDALCO, Jharkhand, India; PG was achieved from Paradip Phosphate Limited in Bhubaneswar, India; and GGBS was collected from TATA steel Jamshedpur. The specific gravity of BR, PG and GGBS were measured as 3.16, 2.78, and 2.94, respectively. The major oxide constituents of each material are provided in Table 1. To conduct the experiment, NaOH with 99% purity and sodium silicate with 99% purity were used. Sand was collected from the Kharkai river and met the specifications of zone II, with a maximum dimension of 4.75 mm and a specific gravity of 2.71 (IS:383, 1970). Coarse aggregate with a specific gravity of 2.78 and a maximum dimension of 20 mm was also used.

Mix design

Geopolymer concrete was developed using BR, PG and GGBS as the precursor material. Before testing, an adequate amount of BR, PG and GGBS were air dried and passed through a 75 μm sieve. Different proportions of PG and GGBS were substituted for BR, as represented in Table 2. To determine the optimal alkali to binder ratio, a preliminary test was conducted, and the optimum ratio was found to be 0.5 after several trials. The alkali proportion in the ratio refers to the combined mass of Na_2SiO_3 and NaOH. The ratio of Na_2SiO_3 to NaOH remained constant at 1.5 in all mixtures, with a NaOH concentration of 12 M. The mix design for each cubic meter of geopolymer is presented in Table 2. The dry mixture of BR, PG, GGBS, coarse aggregate, and fine aggregate was mixed for 4 min before adding the alkali solution and mixing 3 min with alkali solution. The curing of all specimens was done at

Table 1 Oxides compositions

Oxides compositions	BR	PG	GGBS
SiO_2	17.32	7.82	30.24
Fe_2O_3	36.45	0.53	10.45
Al_2O_3	16.36	5.13	14.61
CaO	2.18	38.01	33.38
Na_2O	14.71	0.25	0.78
TiO_2	8.11	–	0.84
K_2O	0.37	–	0.52
SO_3	0.19	42.37	1.57
P_2O_5	0.43	1.3	–
MgO	0.20	0.21	4.85
Loss on ignition (LOI)	3.68	4.38	2.76

Table 2 Mix design of GPC

Mix ID	BR + PG + GGBS = 410 (Kg/m ³)			Coarse aggregate (CA) (Kg/m ³)	Fine aggregate (FA) (Kg/m ³)	NaOH (Kg/m ³)	Na ₂ SiO ₃ (Kg/m ³)
	BR (%)	PG (%)	GGBS (%)				
B1	80	10	10	1145	655	76	114
B2	70	10	20	1145	655	76	114
B3	70	20	10	1145	655	76	114
B4	60	10	30	1145	655	76	114
B5	60	20	20	1145	655	76	114
B6	60	30	10	1145	655	76	114
B7	50	10	40	1145	655	76	114

65 °C for 24 h after casting, and then demoulded and put at ambient temperature for curing till the testing periods.

Tests

Fresh properties

The workability test is conducted according to the Indian Standard (IS) 1199-1959 (Reaffirmed 2004), which specifies the procedure for determining the slump of concrete (IS:1199-1959(Reaffirmed2004) 2004). The test is performed immediately after the mixing of all constituents of the concrete. When conducting a slump test on GPC, it is important to place the material into the moulds immediately after the test to avoid the loss of workability, as GPC tends to set quickly.

Mechanical properties

The compressive strength, flexural strength and split tensile strength were carried out by casting cube of dimension 150 mm × 150 mm × 150 mm, prism of size 100 mm × 100 mm × 500 mm and cylindrical samples of size 150 mm diameter × 300 mm height, respectively as per the IS:10086 (2004) standard. The samples tested for curing period 3 days, 7 days and 28 days. The test is performed on an average of three samples, and the results are reported in megapascals (MPa).

Durability test

Rapid chloride penetration test (RCPT) has been tested as per (ASTM C, 1202 2012), whereas ASTM C 642 is used to evaluate the porosity and water absorption of GPC (ASTM C642, 2013). The RCPT, porosity and water absorption were tested after 28 days cured specimens of the GPC. The RCPT measures the resistance of concrete against chloride ion penetration, which is a major cause of corrosion in concrete structures. The RCPT involves creating a small electrical circuit between a concrete specimen and a solution containing chloride ions. The specimen is then subjected to

an electrical charge, and the amount of charge that passes through the concrete is measured. The test is conducted for a set duration, usually 6 h. Water absorption testing involves submerging a sample of the material in water for 24 h, and then weighing it to determine how much water has been absorbed. Porosity testing, on the other hand, involves measuring the amount of void space in the material, which can affect its overall strength and durability. This test can be done by measuring the weight and volume of the material, and then calculating the percentage of pore space.

Microstructure analysis

Morphological and microstructure characteristics of specimens were investigated using scanning electron microscope (SEM) (ZEISS, Germany). Samples in their powder form is passing through 75 microns sieve and dried at 105 °C for 24 h, were employed for analysis purpose. Prior to analysis, each sample was coated with gold to reveal the best morphology and microstructure features (Mishra et al., 2020). For detecting the governing minerals in samples, D8 discover (make, Bruker, Germany) X-ray diffraction (XRD) was used. All the mineralogical features were established on powder samples passing 75-micron sieve and dried at 105 °C before subjected to testing (Mishra et al., 2020).

Results and discussion

Slump test

Figure 1 illustrates the experimental results of slump values for various mixes of GPC. The results indicate that mix B7 has the lowest slump value of 55 mm, while mix B1 has the maximum slump value of 97 mm. The slumps of B1, B2, B3, B4, B5, B6 and B7 are 97 mm, 94 mm, 88 mm, 77 mm, 80 mm, 63 mm, and 65 mm, respectively. This suggests that the B7 mix is more resistant to deformation and has a higher viscosity compared to B1, which is more fluid and has a lower viscosity. This variation in slump values can be attributed to the differences in the proportions of the mixes. Mix

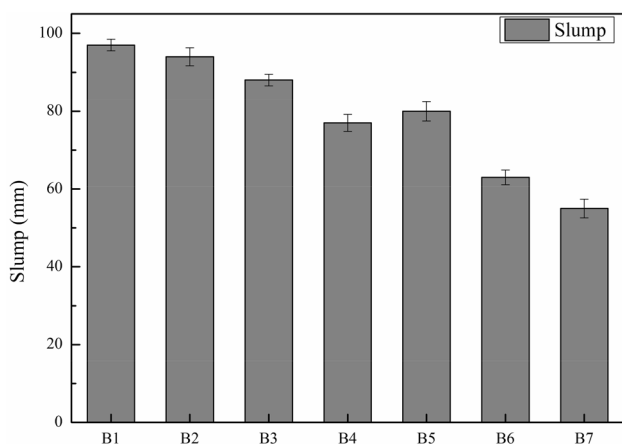


Fig. 1 Slump of fresh GPC

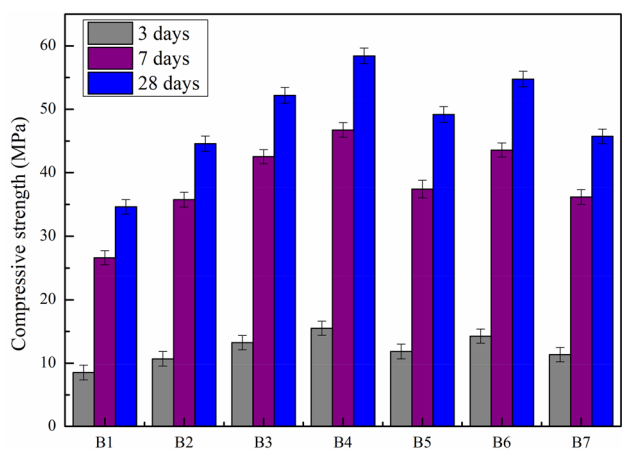


Fig. 2 Compressive strength of GPC

B7 contains a higher proportion of PG and GGBS, which reduce the slump. The presence of PG and GGBS in the mix results in a lower water demand and increased resistance to deformation, leading to a lower slump value (Chen et al., 2021; Xu & Shi, 2018). In contrast, mixes B1 and B2 have a higher slump value, indicating a more fluid consistency. This is likely due to the higher content of BR in these mixes (Chen et al., 2021; Jothilingam & Preethi, 2021).

Compressive strength

Figure 2 displays the compressive strength of GPC for 3 days, 7 days and 28 days. The outcomes depict that the compressive strength of all GPC mixes increases with time. This rise in strength is due to the ongoing geopolymerization process and the continued development of the binding matrix in the concrete (Amran et al., 2020; Bellum et al., 2020; Hamdane et al., 2020). The rate of strength improvement was observed to be faster in the early days of curing,

and the rate of increase slowed down as the curing time progressed. At 28 days, the compressive strength of GPC was resulted to be higher than its strength at 3 days or 7 days, indicating the importance of the curing time for achieving higher strength. The compressive strength of the geopolymer at 28 days for B1, B2, B3, B4, B5, B6 and B7 is 34.61 MPa, 44.57 MPa, 52.18 MPa, 58.42 MPa, 49.18 MPa, 54.76 MPa and 45.73 MPa, respectively. These mixes varied in the amount and type of materials used, such as bauxite residue (BR), phosphogypsum (PG), and GGBS. The maximum compressive strength was obtained when the bauxite residue was replaced with 10% phosphogypsum and 30% GGBS. The compressive strength of this mix, B4, was 58.42 MPa at 28 days. This indicates that the incorporation of PG and GGBS improved the strength development of GPC.

The strength development of GPC is attributed to the process of geopolymerization, which implicates the reaction of aluminosilicate materials in alkaline solution to form a geopolymeric gel (Alam et al., 2019; Nie et al., 2019; Prasanphan et al., 2019). The geopolymeric gel provides the binding matrix in the concrete and contributes to its strength development (Hu et al., 2018; Zhao et al., 2019). However, when the amount of PG or GGBS was increased to 40%, the compressive strength of GPC reduced. This decline in strength may be due to the excess amount of calcium based materials, which could negatively affect the geopolymerization process (Nuaklong et al., 2019). Excessive amounts of PG or GGBS could result in the development of weak spots in the geopolymeric gel, prominent to a reduction in strength.

Flexural strength

Flexural strength is crucial in structural applications such as beams, columns, and slabs. It determines the ability of geopolymer concrete to resist bending loads, dead loads, live loads, and several external forces. High flexural strength ensures the structural safety of the infrastructure (Badkul et al., 2021). The outcomes presented in Fig. 3 illustrate the flexural strength of GPC mixes at curing period of 3 days, 7 days, and 28 days. Similar pattern can be seen in flexural strength as the compressive strength. This study reveals that the flexural strength of each mix enhanced with time due to the ongoing hydration reaction (Verma & Dev, 2021). As the reaction progresses, the strength of the GPC increases. The flexural strength of GPC at 28 days for seven different mixes (B1 to B7) was measured and recorded. The flexural strength of the GPC at 28 days for B1, B2, B3, B4, B5, B6 and B7 are 5.53 MPa, 6.14 MPa, 7.12 MPa, 7.62 MPa, 6.46 MPa, 7.45 MPa and 7.36 MPa, respectively. The outcomes show that the maximum flexural strength was obtained when the bauxite residue was replaced with 10% PG and 30% GGBS. The results indicate that when the phosphogypsum or GGBS

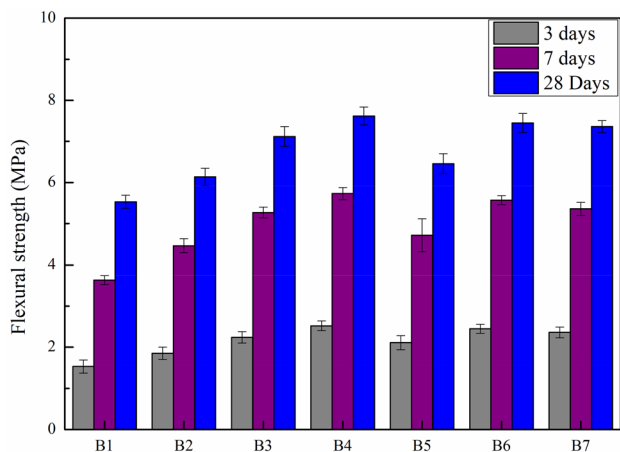


Fig. 3 Flexural strength at different mix compositions

was added up to 30%, the flexural strength of the GPC raised. However, when the amount of phosphogypsum or GGBS was increased to 40%, the flexural strength was reduced. This could be due to the fact that an excessive amount of these materials can cause a dilution effect, causing in a lower concentration of the binding matrix and, therefore, lower flexural strength (Hertel & Pontikes, 2020). As per IRC: 58 (2015) minimum flexural strength of the concrete should be 4.5 MPa for the construction of rigid pavement (IRC: 58 2015). The obtained flexural strength of all the geopolymer concrete is more than 4.5 MPa, so that geopolymer concrete can be used for the construction of pavement (Badkul et al., 2021). It can be used as sustainable development materials which can reduce the CO₂ emissions (Kaveh et al., 2022).

Split tensile strength

Figure 4 shows the split tensile strength of GPC at different duration (3 days, 7 days, and 28 days). The growth in

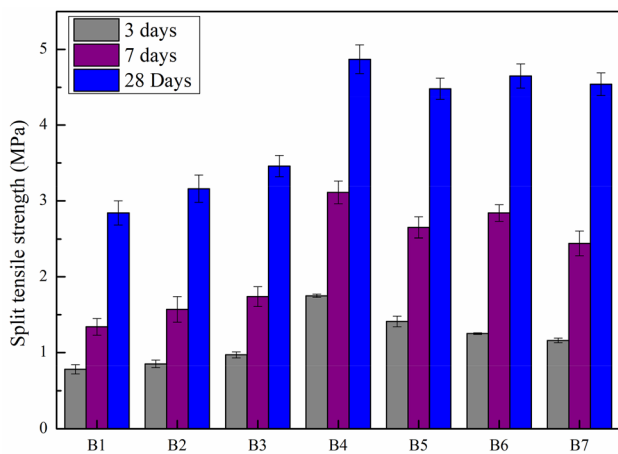


Fig. 4 Split tensile strength at different mix compositions

split tensile strength with curing time is alike to the pattern seen in compressive strength, another important parameter in concrete strength evaluation. Mixes B1, B2, B3, B4, B5, B6, and B7 had split tensile strengths of 2.84 MPa, 3.16 MPa, 3.46 MPa, 4.87 MPa, 4.48 MPa, 4.65 MPa, and 4.54 MPa, respectively. The results indicate that small variations were obtained in mixes B1, B2, and B3. The maximum split tensile strength was obtained when the bauxite residue was replaced with 10% phosphogypsum and 30% GGBS. This indicates that the combination of phosphogypsum and GGBS is effective in enhancing the strength of GPC. This finding is reliable with previous researchers have shown the beneficial effects of GGBS on the strength of GPC owing to its pozzolanic characteristics (Hua et al., 2016; Ngarm et al., 2015; Phoo-ngernkham et al., 2014).

Relation among compressive strength, flexural strength and split tensile strength

This section discusses the correlation between compressive strength, flexural strength, and split tensile strength of geopolymer concrete, with a focus on their 28-day strength properties.

It can be useful to predict the flexural and split tensile strength from the resulted compressive strength (Kaveh & Khalegi, 1998; Kaveh & Khavaninzadeh, 2023). The results were then represented graphically in Figs. 5 and 6. Figure 5 illustrates the correlation between compressive strength and flexural strength, while Fig. 6 shows the relationship between compressive strength and split tensile strength. These figures provide equations that agree the determination of the flexural strength and split tensile strength of geopolymer concrete based on its compressive strength and similar results have been observed by Badkul et al. (2021). By utilizing the equations provided in these figures, the flexural

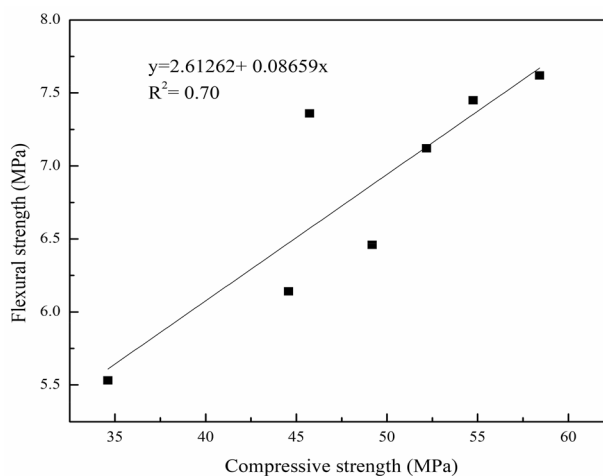


Fig. 5 Relation between compressive strength vs flexural strength

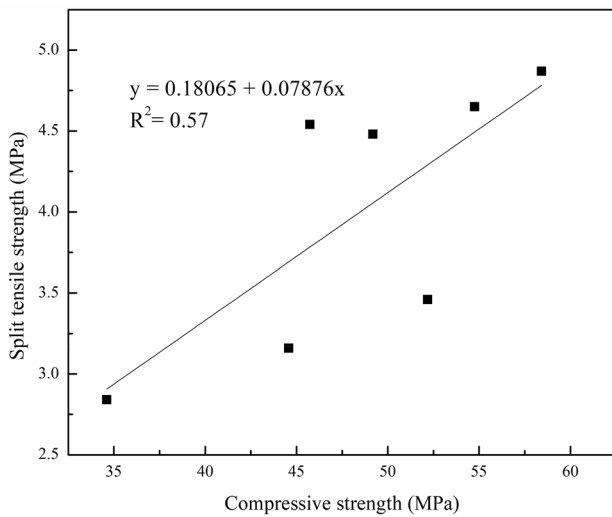


Fig. 6 Relation between compressive strength vs split tensile strength

strength (from Fig. 5) and split tensile strength (from Fig. 6) of geopolymer concrete can be calculated when the compressive strength is known.

Durability test

RCPT test

Figure 7 illustrates the variation of charge passed measured with geopolymer specimen. The electrical conductivity of B1, B2, B3, B4, B5, B6 and B7 are 2846, 2478, 1936, 1575, 2285, 1675 and 2354 Coulomb respectively. The outcome shows that the RCPT test is opposite to the strength of the GPC. The higher strength shows the lower RCPT values. In other words, the higher the strength of the concrete, the lower the charge passed value, indicating better durability against chloride ion penetration. This is a desirable

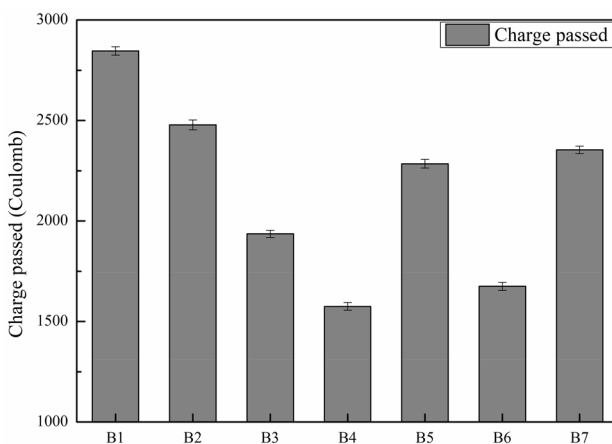


Fig. 7 RCPT test of different mix compositions

characteristic for concrete used in harsh environments, such as marine structures, where the concrete is exposed to high levels of chloride ions (Adesina, 2020; Chen et al., 2021; Jindal & Sharma, 2020). The lowest charge passed is 1575 Coulomb was obtained when the bauxite residue was replaced with 10% phosphogypsum and 30% GGBS. Also, the minimum chloride penetration can be observed when the BR was replaced with 30% PG and 10% GGBS. PG and GGBS can help in the formation of the C–A–S–H and sodium aluminosilicate hydrate (N–A–S–H) gel due to the calcium oxide in alkaline solution (Jindal & Sharma, 2020). The addition of the PG and GGBS to the bauxite residue causes to increase the density and reduces the pores of the geopolymer which leads to reduction in chloride ions penetrations (Chen et al., 2021). This result suggests that the addition of phosphogypsum and GGBS can improve the durability of GPC. The use of by-products such as phosphogypsum and GGBS can further enhanced the durability of GPC, which develop a more sustainable and durable construction material.

Water absorption and porosity test

Figure 8 shows the water absorption and porosity of the GPC after 28 days of the curing periods. Porosity and water absorption both show the similar pattern. The results show that replacing bauxite residue with 10% phosphogypsum and 10% GGBS (B1) resulted in a porosity of 13.42% and water absorption of 5.62%. When the bauxite residue was replaced with 10% phosphogypsum and 30% GGBS (B4), the porosity and water absorption were reduced to 7.53% and 3.15%, respectively. The results indicate that the geopolymer with B4 has a less porosity and water absorption compared to the geopolymer with B1. The decrease in porosity and water absorption can be owing to the addition of PG and GGBS. At a constant 10% PG, when a lesser amount of GGBS is

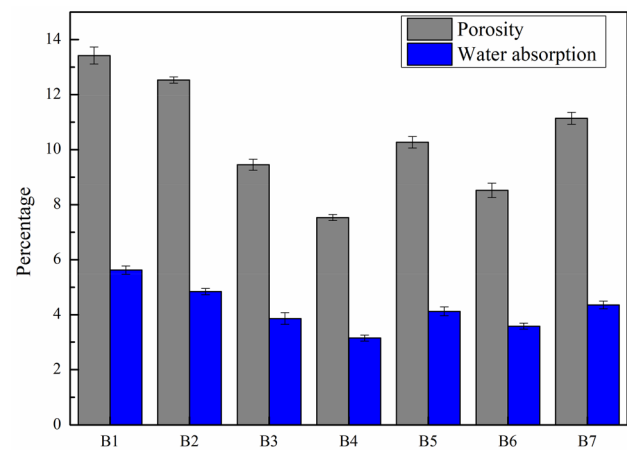


Fig. 8 Porosity and water absorption of different mix compositions

added, less gel will be formed due to the presence of silica oxides in GGBS. On the other hand, at a constant 10% PG, when 30% GGBS is added, more gel will be formed, reducing the number of pores (Alam et al., 2019). As a result, both porosity and water absorption are decreased. These materials can contribute to the generation of C–A–S–H and N–A–S–H gel due to the calcium oxide in alkaline solution (Jindal & Sharma, 2020). The formation of these gels helps to fill the pores in the specimen and reduce its porosity. The reduced porosity also results in a lower water absorption rate (Sam-bangi & Eluru, 2023).

Microstructure analysis

SEM

The three SEM images labeled as Figs. 9, 10, and 11, which illustrate the microstructure of a geopolymer concrete. In Fig. 9, the SEM micrograph displays the surface of the GPC mix, which includes PG and GGBS particles replaced the BR with 10%. The image indicates that there are visible BR particles on the surface, but there is no evidence of gel formation. This implies that there is no proper formation of gel in this sample. Gel formation is essential in geopolymerization because it acts as a binding agent that holds the particles together to form a dense matrix (Wang et al., 2020). In contrast, Fig. 10 illustrates a dense matrix that resulted from the proper development of gel (C–A–S–H and N–A–S–H) due to the addition of the PG and GGBS in alkali solution of the GPC mix (Ma et al., 2022; Zhou et al., 2020). The image shows that the alkali-activated 10% PG and 30% GGBS exhibit a denser structure than the other specimens. This indicates that the PG and GGBS proportions have a remarkable impact on

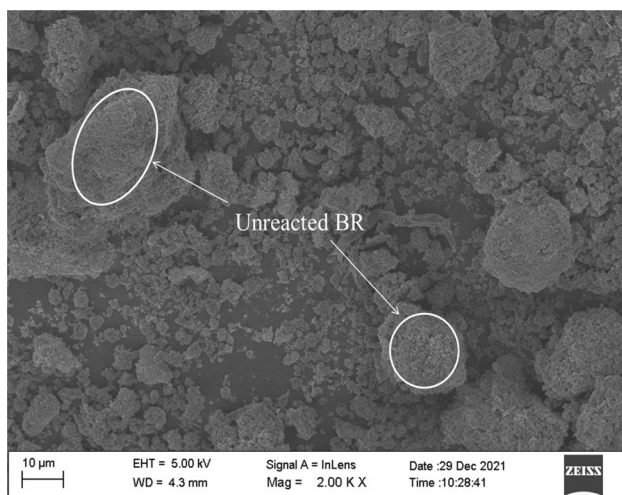


Fig. 9 SEM micrograph of geopolymer with BR: PG: GGBS ratio of 80:10:10 (B1)

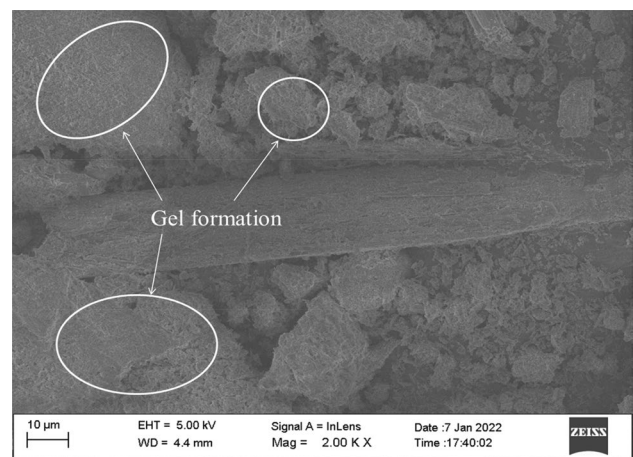


Fig. 10 SEM micrograph of geopolymer with BR: PG: GGBS ratio of 60:10:30 (B4)

the structure and strength of the GPC. The 10% PG and 30% GGBS content resulted in a denser matrix, indicating better gel formation and a higher strength GPC. It is true with Figs. 2, 3, and 4 that show maximum strength for B4. Figure 11 depicts a loose structure, which indicates incomplete gel formation in the GPC. Incomplete gel formation is due to insufficient gel formation, which is crucial in the geopolymerization process (Alam et al., 2019; Sudhir et al., 2020). The image shows that there is a lack of cohesion and bonding between the particles, resulting in a loose structure that is weaker and less durable. Moreover, the statement also mentions that the B4 samples have fewer pores than the B7 samples, which clues to enhance in compressive strength. B4 samples have better quality, resulting in a denser and stronger structure than B1 and B7 samples.

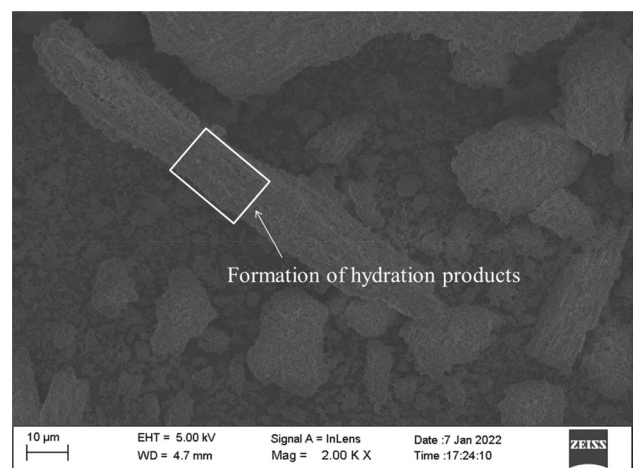


Fig. 11 SEM micrograph of geopolymer with BR: PG: GGBS ratio of 50:10:40 (B7)

XRD

To illustrate the consequence of GGBS blended with BR and PG on the GPC, B1, B4 and B7 specimens were selected for XRD tests. Figure 12 presents the XRD pattern of GPC which shows the presence of hematite, C–A–S–H gel, gibbsite, N–A–S–H gel, ettringite, calcite and gypsum. The wide humps observed at 30° – 35° suggest the presence of calcite in the GPC. The peak of calcite is found to increase in B4 as compared to B1, which indicates that the maximum strength of the GPC is attained in the B4 mix. However, in the B7 mix, the peak of calcite is reduced, which confirms that the strength of the GPC also decreases in this mix. The XRD test also shows the presence of an amorphous phase at 25° , which is found to increase. This increase may be due to the transformation of gels into ettringite, a hydration product that can contribute to rise in the strength of the GPC specimens when present in the proper amount (Aminul Haque et al., 2020; Kaya & Soyer-Uzun, 2016; Zhang et al., 2020a). The C–A–S–H gel can be also observed that its peak increased in B4 that can be confirmed from Figs. 2, 3, and 4 that give maximum strength for the mix B4. On the other hand, a decrease in the peak intensity of ettringite and N–A–S–H gel is seen in the B7 mix, indicating that the strength of the GPC is reduced in this mix (Hu et al., 2019; Li et al., 2021a, b; Xu et al., 2022). The reduction in ettringite peak intensity may be due to the incomplete formation of this hydration product, which can affect the strength of the GPC. The decrease in N–A–S–H gel peak intensity may be due to the reduction in the amount of BR and PG in the mix. The XRD results suggest that the mixture of GGBS, BR, and PG with GPC affects the hydration products and consequently the strength of the concrete. The occurrence of calcite, C–A–S–H gel, ettringite, and N–A–S–H gel is observed in all mixes, but their peak intensities vary depending on the mix composition.

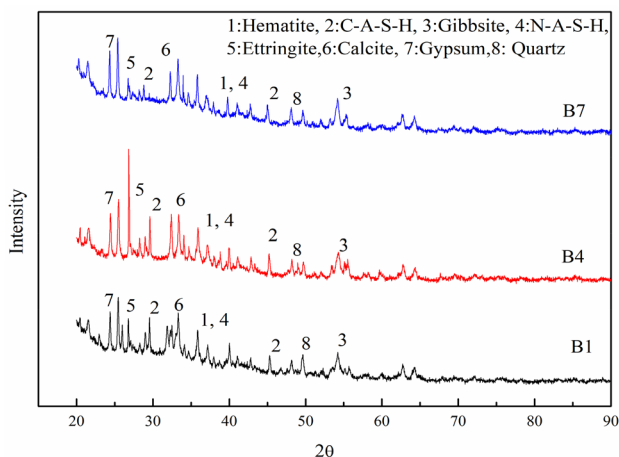


Fig. 12 XRD pattern of geopolymer concrete

Conclusions

The study presented here showcases the creation and advancement of GPC through the utilization of BR, PG, and GGBS, which are typically classified as waste materials and often disposed of in landfills. The comprehensive experimentation and analysis conducted in this research have yielded the subsequent conclusions.

- According to the findings, replacing the bauxite residue with 10% phosphogypsum and 30% GGBS (B4) achieve maximum compressive strength, which was 58.42 MPa. The flexural strength and split tensile strength of mix B4 were 7.62 MPa and 4.87 MPa, respectively.
- The outcomes indicate that the addition of up to 30% GGBS and 10% PG increased the strength of the GPC and led to a denser matrix with reduced porosity and water absorption. This denser matrix resulted in a decrease in chloride ion penetration, water absorption and porosity of the GPC.
- SEM images depicted that the inclusion of PG and GGBS in the alkali solution of the GPC mix resulted in formation of C–A–S–H and N–A–S–H gel, which led to a denser structure in the alkali-activated 10% PG and 30% GGBS specimens compared to other mixes.
- The XRD results showed that the mixture of GGBS, bauxite residue, and phosphogypsum affected the hydration products and consequently the strength of the concrete. The presence of calcite, C–A–S–H gel, ettringite, and N–A–S–H gel was observed in all mixes, but their peak intensities varied depending on the mix composition.
- The measured strength perfectly suits for construction work and remarkably satisfies the necessity as a substitute to cement concrete.

Author contributions BP: Methodology, Investigation, Writing—original draft. SM: Writing—review, editing and Supervision. BHR: Conceptualization, Methodology, editing and Supervision.

Funding No funding to declare.

Data availability Data related to this study may be made available on reasonable request from the corresponding author.

Declarations

Conflict of interest The authors declare that there is no conflict of interest regarding the publication of this paper.

References

- Adesina, A. (2020). Performance of fibre reinforced alkali-activated composites—A review. *Materialia*. <https://doi.org/10.1016/j.mtla.2020.100782>
- Alam, S., Das, S. K., & Rao, B. H. (2019). Strength and durability characteristic of alkali activated GGBS stabilized red mud as geo-material. *Construction and Building Materials*, *211*, 932–942. <https://doi.org/10.1016/j.conbuildmat.2019.03.261>
- AminulHaque, M., Chen, B., Liu, Y., Farasat Ali Shah, S., & Ahmad, M. R. (2020). Improvement of physico-mechanical and microstructural properties of magnesium phosphate cement composites comprising with phosphogypsum. *Journal of Cleaner Production*, *261*, 121268. <https://doi.org/10.1016/j.jclepro.2020.121268>
- Amran, Y. H. M., Alyousef, R., Alabduljabbar, H., & El-Zeadani, M. (2020). Clean production and properties of geopolymer concrete; A review. *Journal of Cleaner Production*. <https://doi.org/10.1016/j.jclepro.2019.119679>
- ASTM C1202. (2012). Standard test method for electrical indication of concrete's ability to resist chloride ion penetration. *American Society for Testing and Materials* 100(C): 1–8. <https://doi.org/10.1520/C1202-12.2>
- ASTM C 642-13. (2013). Standard test method for density, absorption, and voids in hardened concrete. West Conshohocken, PA, 2013.
- Badkul, A., Paswan, R., Singh, S. K., & Tegar, J. P. (2021). A comprehensive study on the performance of alkali activated fly ash/GGBFS geopolymer concrete pavement ash/GGBFS geopolymer concrete pavement. *Road Materials and Pavement Design*. <https://doi.org/10.1080/14680629.2021.1926311>
- Bellum, R. R., Muniraj, K., & Madduru, S. R. C. (2020). Characteristic evaluation of geopolymer concrete for the development of road network: Sustainable infrastructure. *Innovative Infrastructure Solutions*. <https://doi.org/10.1007/s41062-020-00344-5>
- Chen, K., Wu, D., Xia, L., Cai, Q., & Zhang, Z. (2021). Geopolymer concrete durability subjected to aggressive environments—A review of influence factors and comparison with ordinary Portland cement. *Construction and Building Materials*, *279*, 122496. <https://doi.org/10.1016/j.conbuildmat.2021.122496>
- Hamdane, H., Tamraoui, Y., Mansouri, S., Oumam, M., Bouih, A., El Ghailassi, T., Boulif, R., Manoun, B., & Hannache, H. (2020). Effect of alkali-mixed content and thermally untreated phosphate sludge dosages on some properties of metakaolin based geopolymer material. *Materials Chemistry and Physics*, *248*, 122938. <https://doi.org/10.1016/j.matchemphys.2020.122938>
- Hertel, T., & Pontikes, Y. (2020). Geopolymers, inorganic polymers, alkali-activated materials and hybrid binders from bauxite residue (red mud)—Putting things in perspective. *Journal of Cleaner Production*, *258*, 120610. <https://doi.org/10.1016/j.jclepro.2020.120610>
- Hoang, M. D., Do, Q. M., & Le, V. Q. (2020). Effect of curing regime on properties of red mud based alkali activated materials. *Construction and Building Materials*, *259*, 119779. <https://doi.org/10.1016/j.conbuildmat.2020.119779>
- Hu, W., Nie, Q., Huang, B., Shu, X., & He, Q. (2018). Mechanical and microstructural characterization of geopolymers derived from red mud and fly ashes. *Journal of Cleaner Production*, *186*, 799–806. <https://doi.org/10.1016/j.jclepro.2018.03.086>
- Hu, Y., Liang, S., Yang, J., Chen, Y., Ye, N., Ke, Y., Tao, S., Xiao, K., Hu, J., Hou, H., Fan, W., Zhu, S., Zhang, Y., & Xiao, B. (2019). Role of Fe species in geopolymer synthesized from alkali-thermal pretreated Fe-rich Bayer red mud. *Construction and Building Materials*, *200*, 398–407. <https://doi.org/10.1016/j.conbuildmat.2018.12.122>
- Hua, S., Wang, K., & Yao, X. (2016). Developing high performance phosphogypsum-based cementitious materials for oil-well cementing through a step-by-step optimization method. *Cement and Concrete Composites*, *72*, 299–308. <https://doi.org/10.1016/j.cemconcomp.2016.05.017>
- IRC: 58. (2015). *Guidelines for the design of plain jointed rigid pavements for highways*. Indian Road Congress
- IS:10086. (2004) Indian Standard Specification for Moulds for Use in Tests of Cement and Concrete, Edition 1.5, Bureau of Indian Standards, New Delhi, India, 2004
- IS:1199-1959(Reaffirmed2004). (2004). *Methods of sampling and analysis of concrete cement* (pp. 1–49). <https://doi.org/10.2174/18722105130103>.
- IS:383. (1970). Specification for coarse and fine aggregates from natural sources for concrete. In *Indian Standard* (pp. 1–24). Bureau of Indian Standards, New Delhi, India
- Jatoliya, A., Saha, S., Pratap, B., & Mondal, S. (2023). Assessment of bauxite residue stabilized with lime and graphene oxide as a geomaterial for road applications. *Soils and Rocks*, *46*(1), 1–13.
- Jindal, B. B., & Sharma, R. (2020). The effect of nanomaterials on properties of geopolymers derived from industrial by-products: A state-of-the-art review. *Construction and Building Materials*, *252*, 119028. <https://doi.org/10.1016/j.conbuildmat.2020.119028>
- Jothilingam, M., & Preethi, V. (2021). Feasibility, compressive strength and utilization of redmud in geopolymer concrete for sustainable constructions. *Materials Today: Proceedings*. <https://doi.org/10.1016/j.matpr.2021.01.535>
- Kaveh, A., & Khalegi, A. (1998). Prediction of strength for concrete specimens using artificial neural network. *Asian Journal of Civil Engineering*, *2*(2), 1–13.
- Kaveh, A., & Khavaninzadeh, N. (2023). Efficient training of two ANNs using four meta-heuristic algorithms for predicting the FRP strength. *Structures*, *52*, 256–272. <https://doi.org/10.1016/j.istruc.2023.03.178>
- Kaveh, A., Mottaghi, L., & Izadifard, R. A. (2022). Sustainable design of reinforced concrete frames with non-prismatic beams. *Engineering with Computers*, *38*(1), 69–86. <https://doi.org/10.1007/s00366-020-01045-4>
- Kaya, K., & Soyer-Uzun, S. (2016). Evolution of structural characteristics and compressive strength in red mud-metakaolin based geopolymer systems. *Ceramics International*, *42*(6), 7406–7413. <https://doi.org/10.1016/j.ceramint.2016.01.144>
- Li, S., Zhang, J., Li, Z., Gao, Y., & Liu, C. (2021a). Feasibility study of red mud-blast furnace slag based geopolymeric grouting material: Effect of superplasticizers. *Construction and Building Materials*, *267*, 120910. <https://doi.org/10.1016/j.conbuildmat.2020.120910>
- Li, Y., Liu, X., Li, Z., Ren, Y., Wang, Y., & Zhang, W. (2021b). Preparation, characterization and application of red mud, fly ash and desulfurized gypsum based eco-friendly road base materials. *Journal of Cleaner Production*, *284*, 124777. <https://doi.org/10.1016/j.jclepro.2020.124777>
- Liang, X., & Ji, Y. (2021). Mechanical properties and permeability of red mud-blast furnace slag-based geopolymer concrete. *SN Applied Sciences*, *3*(1), 1–10. <https://doi.org/10.1007/s42452-020-03985-4>
- Liu, Q., Cui, M., Li, X., Wang, J., Wang, Z., Li, L., & Lyu, X. (2022). Alkali-hydrothermal activation of mine tailings to prepare one-part geopolymer: Activation mechanism, workability, strength, and hydration reaction. *Ceramics International*. <https://doi.org/10.1016/j.ceramint.2022.06.318>
- Ma, F., Chen, L., Lin, Z., Liu, Z., Zhang, W., & Guo, R. (2022). Microstructure and key properties of phosphogypsum-red mud-slag composite cementitious materials. *Materials (Basel)*, *15*(17), 1–18. <https://doi.org/10.3390/ma15176096>

- Meskini, S., Remmal, T., Ejjaouani, H., & Samdi, A. (2022). Formulation and optimization of a phosphogypsum—fly ash—lime composite for road construction: A statistical mixture design approach. *Construction and Building Materials*, 315, 125786. <https://doi.org/10.1016/j.conbuildmat.2021.125786>
- Mishra, M. C., Reddy, N. G., & Rao, B. H. (2020). Potential of citric acid for treatment of extremely alkaline bauxite residue: Effect on geotechnical and geoenvironmental properties. *Journal of Hazardous, Toxic, and Radioactive Waste*, 24(4), 04020047. [https://doi.org/10.1061/\(asce\)hz.2153-5515.0000541](https://doi.org/10.1061/(asce)hz.2153-5515.0000541)
- Naenudon, S., Wongsas, A., Ekprasert, J., Sata, V., & Chindaprasirt, P. (2023). Enhancing the properties of fly ash-based geopolymer concrete using recycled aggregate from waste ceramic electrical insulator. *Journal of Building Engineering*, 68, 106132. <https://doi.org/10.1016/j.job.2023.106132>
- Ngarm, P., Chindaprasirt, P., & Sata, V. (2015). Setting time, strength, and bond of high-calcium fly ash geopolymer concrete. *Journal of Materials in Civil Engineering*, 27(7), 04014198. [https://doi.org/10.1061/\(asce\)mt.1943-5533.0001157](https://doi.org/10.1061/(asce)mt.1943-5533.0001157)
- Nie, Q., Hu, W., Huang, B., Shu, X., & He, Q. (2019). Synergistic utilization of red mud for flue-gas desulfurization and fly ash-based geopolymer preparation. *Journal of Hazardous Materials*, 369, 503–511. <https://doi.org/10.1016/j.jhazmat.2019.02.059>
- Nuaklong, P., Wongsas, A., Sata, V., Boonserm, K., Sanjayana, J., & Chindaprasirt, P. (2019). Properties of high-calcium and low-calcium fly ash combination geopolymer mortar containing recycled aggregate. *Heliyon*, 5(9), e02513. <https://doi.org/10.1016/j.heliyon.2019.e02513>
- Phoo-ngernkham, T., Chindaprasirt, P., Sata, V., Hanjitsuwan, S., & Hatanaka, S. (2014). The effect of adding nano-SiO₂ and nano-Al₂O₃ on properties of high calcium fly ash geopolymer cured at ambient temperature. *Materials & Design*, 55, 58–65. <https://doi.org/10.1016/j.matdes.2013.09.049>
- Phummiphan, I., Horpibulsuk, S., Rachan, R., Arulrajah, A., Shen, S. L., & Chindaprasirt, P. (2018). High calcium fly ash geopolymer stabilized lateritic soil and granulated blast furnace slag blends as a pavement base material. *Journal of Hazardous Materials*, 341, 257–267. <https://doi.org/10.1016/j.jhazmat.2017.07.067>
- Prasanphan, S., Wannagon, A., Kobayashi, T., & Jiemsirilars, S. (2019). Reaction mechanisms of calcined kaolin processing waste-based geopolymers in the presence of low alkali activator solution. *Construction and Building Materials*, 221, 409–420. <https://doi.org/10.1016/j.conbuildmat.2019.06.116>
- Pratap, B., Mondal, S., & Hanumantha Rao, B. (2023a). Synthesis of alkali activated mortar using phosphogypsum neutralized bauxite residue. *Environmental Geotechnics*. <https://doi.org/10.1680/jenge.22.00104>
- Pratap, B., Shubham, K., Mondal, S., & Hanumantha, B. (2023b). Exploring the potential of neural network in assessing mechanical properties of geopolymer concrete incorporating fly ash and phosphogypsum in pavement applications. *Asian Journal of Civil Engineering*. <https://doi.org/10.1007/s42107-023-00735-w>
- Reddy, N. G., Nongmaithem, R. S., Basu, D., & Rao, B. H. (2020). Application of biopolymers for improving the strength characteristics of red mud waste. *Environmental Geotechnics*. <https://doi.org/10.1680/jenge.19.00018>
- Ren, Z., Wang, L., Wang, H., Liu, S., & Liu, M. (2023). Solidification/stabilization of lead-contaminated soils by phosphogypsum slag-based cementitious materials. *Science of The Total Environment*, 857, 159552. <https://doi.org/10.1016/j.scitotenv.2022.159552>
- Sambangi, A., & Eluru, A. (2023). Role of copper slag on improvement of strength, quality and durability of high—strength self—compacting concrete: An industrial waste. *Asian Journal of Civil Engineering*, 2022, 961–971. <https://doi.org/10.1007/s42107-022-00466-4>
- Shahmansouri, A. A., Nematzadeh, M., & Behnood, A. (2021). Mechanical properties of GGBFS-based geopolymer concrete incorporating natural zeolite and silica fume with an optimum design using response surface method. *Journal of Building Engineering*, 36, 102138. <https://doi.org/10.1016/j.job.2020.102138>
- Sudhir, M. R., Beulah, M., Sasha Rai, P., & Gayathri, G. (2020). A microstructure exploration and compressive strength determination of red mud bricks prepared using industrial wastes. *Materials Today: Proceedings*. <https://doi.org/10.1016/j.matpr.2020.07.171>
- Toniolo, N., Rincón, A., Avadhut, Y. S., Hartmann, M., Bernardo, E., & Boccaccini, A. R. (2018). Novel geopolymers incorporating red mud and waste glass cullet. *Materials Letters*, 219, 152–154. <https://doi.org/10.1016/j.matlet.2018.02.061>
- Verma, M., & Dev, N. (2021). Sodium hydroxide effect on the mechanical properties of flyash-slag based geopolymer concrete. *Structural Concrete*, 22(S1), E368–E379. <https://doi.org/10.1002/suco.202000068>
- Wang, X., Zhang, N., Zhang, Y., Liu, J., Wang, C., & Chu, P. K. (2020). Composite plates utilizing dealcalized red mud, acid leaching slag and dealcalized red mud-fly ash: Preparation and performance comparison. *Construction and Building Materials*, 261, 120495. <https://doi.org/10.1016/j.conbuildmat.2020.120495>
- Xu, G., & Shi, X. (2018). Characteristics and applications of fly ash as a sustainable construction material: A state-of-the-art review. *Resources, Conservation and Recycling*, 136, 95–109. <https://doi.org/10.1016/j.resconrec.2018.04.010>
- Xu, J., Xu, F., Wu, Y., Liu, Y., Yang, F., Jiao, Y., Jiang, Y., Zhu, J., Li, S., Wang, D., & Li, B. (2022). Investigation on properties and mechanism of non-calcined Bayer red mud-phosphogypsum cementitious binder. *Journal of Cleaner Production*. <https://doi.org/10.1016/j.jclepro.2022.134661>
- Zakira, U., Zheng, K., Xie, N., & Birgisson, B. (2023). Development of high-strength geopolymers from red mud and blast furnace slag. *Journal of Cleaner Production*, 383, 135439. <https://doi.org/10.1016/j.jclepro.2022.135439>
- Zhang, J., Li, S., & Li, Z. (2020a). Investigation the synergistic effects in quaternary binder containing red mud, blast furnace slag, steel slag and flue gas desulfurization gypsum based on artificial neural networks. *Journal of Cleaner Production*, 273, 122972. <https://doi.org/10.1016/j.jclepro.2020.122972>
- Zhang, J., Li, S., Li, Z., Gao, Y., Liu, C., & Qi, Y. (2020b). Workability and microstructural properties of red-mud-based geopolymer with different particle sizes. *Advances in Cement Research*. <https://doi.org/10.1680/jadcr.19.00085>
- Zhao, M., Zhang, G., Htet, K. W., Kwon, M., Liu, C., Xu, Y., & Tao, M. (2019). Freeze-thaw durability of red mud slurry-class F fly ash-based geopolymer: Effect of curing conditions. *Construction and Building Materials*, 215, 381–390. <https://doi.org/10.1016/j.conbuildmat.2019.04.235>
- Zhou, W., Shi, X., Lu, X., Qi, C., Luan, B., & Liu, F. (2020). The mechanical and microstructural properties of refuse mud-stone-GGBS-red mud based geopolymer composites made with sand. *Construction and Building Materials*, 253, 119193. <https://doi.org/10.1016/j.conbuildmat.2020.119193>

Publisher's Note Springer Nature remains neutral with regard to jurisdictional claims in published maps and institutional affiliations.

Springer Nature or its licensor (e.g. a society or other partner) holds exclusive rights to this article under a publishing agreement with the author(s) or other rightsholder(s); author self-archiving of the accepted manuscript version of this article is solely governed by the terms of such publishing agreement and applicable law.